This article was downloaded by:
On: *25 January 2011*
Access details: *Access Details: Free Access*
Publisher *Taylor & Francis*
Informa Ltd Registered in England and Wales Registered Number: 1072954 Registered office: Mortimer House, 37-41 Mortimer Street, London W1T 3JH, UK

Liquid Crystals
Publication details, including instructions for authors and subscription information:
http://www.informaworld.com/smpp/title~content=t713926090

On the non-symmetric planar aligned NLC cell

Yang Guo Chen Corresponding author[a]; Zhang Zhi Guo[a]; Li Li[a]; Guan Rong Hua[ab]
[a] Physics Institute of Hebei University of Technology, Tianjin 300 130, PR China [b] North China Electric Power University, Baoding 071 003, PR China

Online publication date: 07 July 2010

To cite this Article Chen Corresponding author, Yang Guo , Guo, Zhang Zhi , Li, Li and Hua, Guan Rong(2003) 'On the non-symmetric planar aligned NLC cell', Liquid Crystals, 30: 12, 1441 — 1447
To link to this Article: DOI: 10.1080/02678290310001621903
URL: http://dx.doi.org/10.1080/02678290310001621903

PLEASE SCROLL DOWN FOR ARTICLE

Full terms and conditions of use: http://www.informaworld.com/terms-and-conditions-of-access.pdf

This article may be used for research, teaching and private study purposes. Any substantial or systematic reproduction, re-distribution, re-selling, loan or sub-licensing, systematic supply or distribution in any form to anyone is expressly forbidden.

The publisher does not give any warranty express or implied or make any representation that the contents will be complete or accurate or up to date. The accuracy of any instructions, formulae and drug doses should be independently verified with primary sources. The publisher shall not be liable for any loss, actions, claims, proceedings, demand or costs or damages whatsoever or howsoever caused arising directly or indirectly in connection with or arising out of the use of this material.

LIQUID CRYSTALS, VOL. 30, NO. 12, DECEMBER 2003, 1441–1447

Taylor & Francis
Taylor & Francis Group

On the non-symmetric planar aligned NLC cell

YANG GUOCHEN*†, ZHANG ZHIGUO†, LI LI† and GUAN RONGHUA†‡

†Physics Institute of Hebei University of Technology, Tianjin 300 130, PR China
‡North China Electric Power University, Baoding 071 003, PR China

(*Received 14 May 2003; accepted 25 July 2003*)

The planar aligned nematic liquid crystal cell with different anchoring for the two substrates (i.e. a non-symmetric NLC cell) is investigated by an analytical method. We deduce the basic equations and the boundary conditions of the tilt angle θ of the LC director. Expressions for threshold and saturation magnetic field are obtained, and numerical results of these two quantities with variation in anchoring parameters of the two substrates are given. A symmetry breaking parameter Δ is introduced and the relations between Δ and applied field, as well as the two sets of anchoring parameters are discussed in detail. A feasible experimental plan for measurement of anchoring strengths of a series of different substrates is proposed.

Downloaded At: 17:05 25 January 2011

1. Introduction

The surface physics of liquid crystals (LCs) is an important topic in LC science [1]. The anchoring action between a LC and a solid surface has been paid much attention. In basic research, a planar aligned nematic liquid crystal (NLC) cell is often used. In most of these investigations, the authors suppose that the anchoring of the two substrates of a cell is identical, and the distribution of directors is symmetrical relative to the middle plane of the LC cell. We call this type of cell a symmetrical NLC cell. However, the cell with different anchoring for the two substrates has received little attention. This type of cell is called a non-symmetric NLC cell. We think that the non-symmetric NLC cell has more scope for new applications.

We investigate the non-symmetric NLC cell analytically. The surface anchoring energy of the modified Rapini–Papoular type [2] is adopted, this is

$$g_{\mathrm{s}}=\frac{1}{2}A\sin^2\theta\left(1+\zeta\sin^2\theta\right) \tag{1}$$

where A is the anchoring strength and ζ is a modification parameter. For the lower substrate we use A_1, ζ_1, and for the higher substrate A_2, ζ_2.

In this paper, we describe the main properties of a non-symmetric planar aligned NLC cell. In § 2, the basic equations and boundary conditions of the tilt angle $\theta(z)$ are derived using rigorous mathematical treatment. There are two sets of fundamental equation and corresponding boundary conditions, one set represents a symmetric LC cell with thickness $2d$ and anchoring parameter A_1, ζ_1; the second set represents another symmetric LC cell with thickness $2l-2d$ and anchoring parameter A_2, ζ_2, where $z=d$ is the place of maximum tilt θ_{m} of the non-symmetric cell. So the non-symmetric cell can be seen as two half-symmetric cells in series. In § 3, rigorous expressions for the threshold and saturation fields are derived analytically. The values of these two quantities are dependant on A_1, ζ_1 and A_2, ζ_2. In § 4, in order to show the characteristic property of a non-symmetric cell, we introduce a symmetry breaking parameter Δ, and define

$$\Delta=\frac{d-l/2}{l/2}=2\frac{d}{l}-1. \tag{2}$$

The relation between Δ and applied field as well as A_1, ζ_1, A_2, ζ_2 are discussed in detail by means of a numerical method. In § 5, as an application example, we propose an experimental plan for the measurement of anchoring strengths of a series of different substrates.

2. The non-symmetric planar aligned NLC cell

In figure 1, we give the theoretical model of a non-symmetric NLC cell. The anchoring energy parameters of top and bottom substrates are, respectively (A_2, ζ_2) and (A_1, ζ_1). The director $\mathbf{n}$ is $\mathbf{n}=(\cos\theta,\ 0,\ \sin\theta)$, $\theta=\theta(z)$. The easy direction is $\mathbf{e}=(1,\ 0,\ 0)$ for both substrates. The applied magnetic field is $\mathbf{H}=(0,\ 0,\ H)$. The surface energy per unit area on bottom and top

*Author for correspondence; e-mail: Yang_gc@hotmail.com

Liquid Crystals ISSN 0267-8292 print/ISSN 1366-5855 online © 2003 Taylor & Francis Ltd
http://www.tandf.co.uk/journals
DOI: 10.1080/02678290310001621903

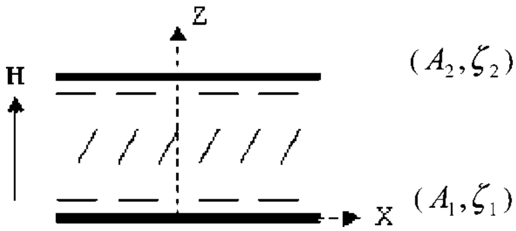

Figure 1. Non-symmetric weak anchoring NLC cell. The anchoring parameters are A_1, ζ_1 (top substrate) and A_2, ζ_2 (bottom substrate).

substrates can be expressed as

$$g_s|_{z=0} = \frac{1}{2} A_1 \sin^2\theta_0 \left(1+\zeta_1 \sin^2\theta_0\right) \tag{3}$$

$$g_s|_{z=l} = \frac{1}{2} A_2 \sin^2\theta_l \left(1+\zeta_2 \sin^2\theta_l\right). \tag{4}$$

The Gibbs free energy [3] per unit volume in the cell can be written

$$g_b = \frac{1}{2}\left(K_{11}\cos^2\theta + K_{33}\sin^2\theta\right)\left(\frac{d\theta}{dz}\right)^2 - \frac{1}{2}\chi_a \mathbf{H}^2 \sin^2\theta \tag{5}$$

where K_{11}, K_{33} are the Frank splay and elastic constants, respectively, and χ_a is the magnetic anisotropy of the NLC medium. The total energy of the system is therefore

$$\begin{aligned} G = S\int_0^l &\left[\frac{1}{2}\left(K_{11}\cos^2\theta + K_{33}\sin^2\theta\right)\left(\frac{d\theta}{dz}\right)^2 \right. \\ &\left. - \frac{1}{2}\chi_a H^2 \sin^2\theta\right] dz + \frac{1}{2} S A_1 \sin^2\theta_0 \\ &\left(1+\zeta_1\sin^2\theta_0\right) + \frac{1}{2} S A_2 \sin^2\theta_l \left(1+\zeta_2 \sin^2\theta_l\right) \end{aligned} \tag{6}$$

where S is the area of the substrate. Applying the calculus of variations [4] of G yields

$$\begin{aligned} &\left(K_{11}\cos^2\theta + K_{33}\sin^2\theta\right)\frac{d^2\theta}{dz^2} - \\ &\left(K_{33}-K_{11}\right)\sin\theta\cos\theta\left(\frac{d\theta}{dz}\right)^2 - \chi_a H^2 \sin\theta\cos\theta = 0. \end{aligned} \tag{7}$$

The boundary conditions at $z=0$ and $z=l$ are, respectively

$$\begin{aligned} &\left(K_{11}\cos^2\theta_0 + K_{33}\sin^2\theta_0\right)\frac{d\theta}{dz}\bigg|_{z=0} \\ &= A_1 \cos\theta_0 \sin\theta_0 \left(1+2\zeta_1 \sin^2\theta_0\right) \end{aligned} \tag{8}$$

$$\begin{aligned} &\left(K_{11}\cos^2\theta_l + K_{33}\sin^2\theta_l\right)\frac{d\theta}{dz}\bigg|_{z=l} \\ &= -A_2 \sin\theta_l \cos\theta_l \left(1+2\zeta_2 \sin^2\theta_l\right). \end{aligned} \tag{9}$$

equation (7) and the boundary conditions (8), (9) have two trivial solutions

$$\theta \equiv \frac{\pi}{2},\ \theta \equiv 0.$$

We call $\theta \equiv 0$ the uniform solution, and $\theta \equiv \pi/2$ the saturation solution. In addition, there is a non-trivial solution, which satisfies

$$\begin{aligned} \frac{1}{2}\frac{d}{dz}&\left[\left(K_{11}\cos^2\theta + K_{33}\sin^2\theta\right)\left(\frac{d\theta}{dz}\right)^2 \right. \\ &\left. + \chi_a \mathbf{H}^2 \sin^2\theta\right] = 0. \end{aligned} \tag{10}$$

The non-trivial solution is named the disturbed solution. From equation (10), we obtain

$$\left(K_{11}\cos^2\theta + K_{33}\sin^2\theta\right)\left(\frac{d\theta}{dz}\right)^2 + \chi_a \mathbf{H}^2 \sin^2\theta = C \tag{11}$$

where C is constant.

We know that when $z=0$, $\frac{d\theta}{dz} > 0$; otherwise when $z=l$, $\frac{d\theta}{dz} < 0$. So there must be a value of $z \in (0, l)$ which satisfies the condition $\frac{d\theta}{dz} = 0$. Putting $z=d$, $\frac{d\theta}{dz}\big|_{z=d} = 0$ and θ has a maximum θ_m. From equation (10), we obtain $C = \chi_a \mathbf{H}^2 \sin^2\theta_m$. Thus equation (11) leads to

$$\begin{aligned} &\left(K_{11}\cos^2\theta + K_{33}\sin^2\theta\right)\left(\frac{d\theta}{dz}\right)^2 = \\ &\chi_a \mathbf{H}^2 \left(\sin^2\theta_m - \sin^2\theta\right) \end{aligned} \tag{12}$$

which can be written as

$$\left(\frac{d\theta}{dz}\right)^2 = \frac{\chi_a \mathbf{H}^2 \left(\sin^2\theta_m - \sin^2\theta\right)}{K_{11}\cos^2\theta + K_{33}\sin^2\theta}. \tag{13}$$

Equation (13) represents two equations, namely

$$\frac{d\theta}{dz} = \left(\frac{\chi_a}{K_{11}}\right)^{\frac{1}{2}} \mathbf{H} \left(\frac{\sin^2\theta_m - \sin^2\theta}{1+\gamma\sin^2\theta}\right)^{\frac{1}{2}},\ \text{for } 0 \leqslant z \leqslant d \tag{14}$$

$$\frac{d\theta}{dz} = -\left(\frac{\chi_a}{K_{11}}\right)^{\frac{1}{2}} \mathbf{H} \left(\frac{\sin^2\theta_m - \sin^2\theta}{1+\gamma\sin^2\theta}\right)^{\frac{1}{2}},\ \text{for } d < z \leqslant l \tag{15}$$

where $\gamma = (K_{33} - K_{11})/K_{11}$.

Substituting equations (14) and (15) into equations (8) and (9), we have the equations of the boundary conditions as

$$\begin{aligned} &\left(K_{11}\chi_a\right)^{\frac{1}{2}} \mathbf{H} \left[\left(1+\gamma\sin^2\theta_0\right)\left(\sin^2\theta_m - \sin^2\theta_0\right)\right]^{\frac{1}{2}} \\ &= A_1 \cos\theta_0 \sin\theta_0 \left(1+2\zeta_1\cos^2\theta_0\right),\ \text{for } z=0 \end{aligned} \tag{16}$$

$$\begin{aligned} &\left(K_{11}\chi_a\right)^{\frac{1}{2}} \mathbf{H} \left[\left(1+\gamma\sin^2\theta_l\right)\left(\sin^2\theta_m - \sin^2\theta_l\right)\right]^{\frac{1}{2}} \\ &= A_2 \cos\theta_l \sin\theta_l \left(1+2\zeta_2\cos^2\theta_l\right),\ \text{for } z=l. \end{aligned} \tag{17}$$

From these equations, we see that equations (14) and

Downloaded At: 17:05 25 January 2011

(16) are the basic equation and boundary condition of a symmetric cell with thickness $2d$ and anchoring parameter A_1, ζ_1. Equations (15) and (17) are the basic equation and boundary condition of a symmetric cell with thickness $2(l-d)$ and anchoring parameter A_2, ζ_2. Thus the non-symmetric cell can be seen as two half symmetric cells in series.

Now we make a variable transformation. Put

$$u=\sin^2\theta_{\rm m} \tag{18}$$

and adopt the new variable v to displace θ

$$v=\frac{\tan^2\theta}{\tan^2\theta_{\rm m}}\ \left(v_0=\frac{\tan^2\theta_0}{\tan^2\theta_{\rm m}},\ v_l=\frac{\tan^2\theta_l}{\tan^2\theta_{\rm m}}\right). \tag{19}$$

Furthermore we introduce reduced quantities

$$h=\frac{\mathbf{H}}{\mathbf{H}_{\rm c}^0},\ \alpha_1=\frac{A_1 l}{2K_{11}},\ \alpha_2=\frac{A_2 l}{2K_{11}}$$

where $H_{\rm c}^0=\frac{\pi}{l}\left(\frac{K_{11}}{\chi_{\rm a}}\right)^{\frac{1}{2}}$. Using these quantities, from equations (14) and (15) we have

$$\frac{\pi}{2}h\frac{2d}{l}=I_{1,0},\ \frac{\pi}{2}h\frac{2l-2d}{l}=I_{1,l}$$

where

$$\begin{aligned}I_{1,0}&=\int_{\theta_0}^{\theta_{\rm m}}\left(\frac{1+\gamma\sin^2\theta}{\sin^2\theta_{\rm m}-\sin^2\theta}\right)^{\frac{1}{2}}{\rm d}\theta\\&=\int_{v_0}^{1}\frac{1}{2[v(1-v)]^{\frac{1}{2}}}\frac{[1-u+(1+\gamma)uv]^{\frac{1}{2}}}{1-u+uv}{\rm d}v\end{aligned} \tag{20}$$

$$\begin{aligned}I_{1,l}&=\int_{\theta_l}^{\theta_{\rm m}}\left(\frac{1+\gamma\sin^2\theta}{\sin^2\theta_{\rm m}-\sin^2\theta}\right)^{\frac{1}{2}}{\rm d}\theta\\&=\int_{v_l}^{1}\frac{1}{2[v(1-v)]^{\frac{1}{2}}}\frac{[1-u+(1+\gamma)uv]^{\frac{1}{2}}}{1-u+uv}{\rm d}v.\end{aligned} \tag{21}$$

With these new variables, the equilibrium equations (14), (15) can be represented as

$$\frac{\pi}{2}h\frac{2d}{l}=I_{1,0} \tag{22}$$

$$\frac{\pi}{2}h\frac{2l-2d}{l}=I_{1,l}. \tag{23}$$

From equations (22) and (23), we easily obtain

$$\frac{\pi}{2}h=\frac{1}{2}(I_{1,0}+I_{1,l}). \tag{24}$$

Boundary conditions (16) and (17) can be expressed as

$$\begin{aligned}\frac{\pi}{2}h=\alpha_1&\left(\frac{v_0}{1-v_0}\right)^{\frac{1}{2}}\\&\times\frac{1-u+u(1+2\zeta_1)v_0}{(1-u+uv_0)[1-u+u(1+\gamma)v_0]^{\frac{1}{2}}},\ \text{for } z=0\end{aligned} \tag{25}$$

$$\begin{aligned}\frac{\pi}{2}h=\alpha_2&\left(\frac{v_l}{1-v_l}\right)^{\frac{1}{2}}\\&\times\frac{1-u+u(1+2\zeta_2)v_l}{(1-u+uv_l)[1-u+u(1+\gamma)v_l]^{\frac{1}{2}}},\ \text{for } z=l.\end{aligned} \tag{26}$$

From these equations, we see that for the exchange of α_1, ζ_1 and α_2, ζ_2, the value of h is the same.

3. Threshold field and saturation field

Suppose that at the threshold and saturation points, the director changes continuously with the applied field. That is to say, the transitions are of second order. First we discuss the threshold field $h_{\rm th}$. Put $u=0$, and equations (24), (25) and (26) become

$$\frac{\pi}{2}h_{\rm th}=\frac{1}{2}\left\{\int_{v_0}^{1}\frac{1}{2[v(1-v)]^{\frac{1}{2}}}{\rm d}v+\int_{v_l}^{1}\frac{1}{2[v(1-v)]^{\frac{1}{2}}}{\rm d}v\right\} \tag{27}$$

$$\frac{\pi}{2}h_{\rm th}=\alpha_1\left(\frac{v_0}{1-v_0}\right)^{\frac{1}{2}} \tag{28}$$

$$\frac{\pi}{2}h_{\rm th}=\alpha_2\left(\frac{v_l}{1-v_l}\right)^{\frac{1}{2}}. \tag{29}$$

Equations (28) and (29) yield

$$v_0=\frac{\pi^2h_{\rm th}^2}{4\alpha_1^2+\pi^2h_{\rm th}^2},\ v_l=\frac{\pi^2h_{\rm th}^2}{4\alpha_2^2+\pi^2h_{\rm th}^2}. \tag{30}$$

Substituting equation (30) into equation (27) leads to

$$\cos(\pi h_{\rm th})=\frac{\pi^2h_{\rm th}^2-4\alpha_1\alpha_2}{\left[\left(4\alpha_1^2+\pi^2h_{\rm th}^2\right)\left(4\alpha_2^2+\pi^2h_{\rm th}^2\right)\right]^{\frac{1}{2}}} \tag{31}$$

or

$$\tan(\pi h_{\rm th})=\frac{2\pi h_{\rm th}(\alpha_1+\alpha_2)}{(\pi h_{\rm th})^2-4\alpha_1\alpha_2}. \tag{32}$$

We can see that the value of $h_{\rm th}$ is same for exchanges $\alpha_1\to\alpha_2$ and $\alpha_2\to\alpha_1$, i.e. $h_{\rm th}\ (\alpha_1,\alpha_2)=h_{\rm th}\ (\alpha_2,\alpha_1)$. When $\alpha_1=\alpha_2=\alpha$, equation (32) can be expressed as $\cot\left(\frac{\pi}{2}h_{\rm th}\right)=\frac{\pi}{2\alpha}h_{\rm th}$. This is consistent with literature results [5].

We now discuss the results for different α_1 and α_2 using numerical calculations. Figure 2 shows the relation between the threshold field $h_{\rm th}$ and the reduced anchoring strength α_1, α_2. In figure 2, curves 1, 2, 3, 4

Downloaded At: 17:05 25 January 2011

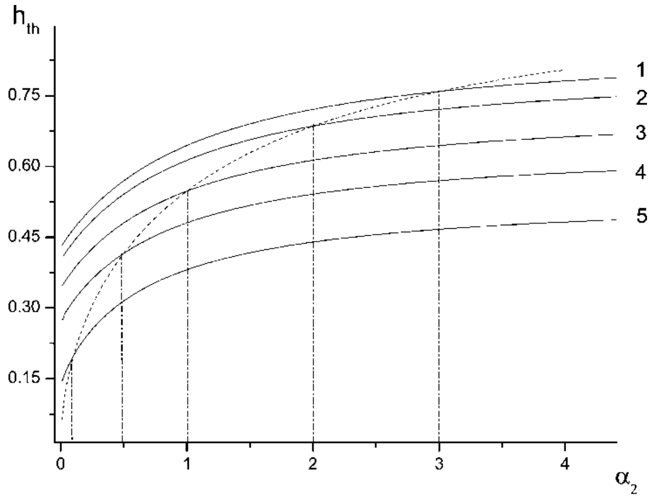

Figure 2. The $h_{th}-\alpha_2$ curves for various α_1. Curves 1, 2, 3, 4 and 5 represent $\alpha_1=3.0$, 2.0, 1.0, 0.5 and 0.1, respectively. The dashed curve represents $\alpha_1=\alpha_2$.

and 5 represent $\alpha_1=3.0$, 2.0, 1.0, 0.5 and 0.1, respectively. The dashed curve represents the case that the values of anchoring strength are same, i.e. $\alpha_1=\alpha_2$. We can see that the value of h_{th} will increase with the increasing of α_1 or α_2; and for fixed α_2, h_{th} increases linearly with α_1.

We next discuss the saturation magnetic field h_s. Putting $u=1$, equations (24), (25) and (26) become

$$\frac{\pi}{2}h_s=\frac{1}{2}\left[\int_{v_0}^{1}\frac{(1+\gamma)^{\frac{1}{2}}}{2v(1-v)}\mathrm{d}v+\int_{v_l}^{1}\frac{(1+\gamma)^{\frac{1}{2}}}{2v(1-v)}\mathrm{d}v\right] \tag{33}$$

$$\frac{\pi}{2}h_s=\alpha_1\frac{1+2\zeta_1}{(1+\gamma)^{\frac{1}{2}}}\frac{1}{(1-v_0)^{\frac{1}{2}}} \tag{34}$$

$$\frac{\pi}{2}h_s=\alpha_2\frac{1+2\zeta_2}{(1+\gamma)^{\frac{1}{2}}}\frac{1}{(1-v_l)^{\frac{1}{2}}}. \tag{35}$$

According to the integral formula $\int\frac{\mathrm{d}x}{x(1-x)^{\frac{1}{2}}}=-2\tanh^{-1}(1-x)^{\frac{1}{2}}$, equation (33) leads to

$$\pi h_s=(1+\gamma)^{\frac{1}{2}}\left[\tanh^{-1}(1-v_0)^{\frac{1}{2}}+\tanh^{-1}(1-v_l)^{\frac{1}{2}}\right]. \tag{36}$$

With equations (33), (34) and (35) and the formula $\tanh(x+y)=\frac{\tanh x+\tanh y}{1+\tanh x\tanh y}$, we obtain

$$\tanh\left[\frac{1}{(1+\gamma)^{\frac{1}{2}}}\pi h_s\right]=\frac{2\pi h_s(1+\gamma)^{\frac{1}{2}}[\alpha_1(1+2\zeta_1)+\alpha_2(1+2\zeta_2)]}{(\pi h_s)^2(1+\gamma)+4\alpha_1\alpha_2(1+2\zeta_1)(1+2\zeta_2)}. \tag{37}$$

We see that h_s is determined by $\alpha_1'=\alpha_1(1+2\zeta_1)$ and $\alpha_2'=\alpha_2(1+2\zeta_2)$, and its value is the same for exchange $\alpha_1'\to\alpha_2'$ and $\alpha_2'\to\alpha_1'$, i.e. $h_s(\alpha_1',\alpha_2')=h_s(\alpha_2',\alpha_1')$. When $\alpha_1=\alpha_2=\alpha$, $\zeta_1=\zeta_2=\zeta$, equation (37) can be simplified to

$$\frac{\pi}{2}h_s=\frac{\alpha(1+2\zeta)}{(1+\gamma)^{\frac{1}{2}}}\coth\left[\frac{1}{(1+\gamma)^{\frac{1}{2}}}\frac{\pi}{2}h_s\right]$$

This is consistent with literature results [6].

We now discuss our results for different α_1' and α_2' using numerical calculations. Figure 3 shows this relation when the value of parameter $\gamma=0.25$ is adopted. Curves 1, 2 and 3 represent $\alpha_1'=0.9$, 0.5 and 0.1, respectively. The dashed curve represents $\alpha_1'=\alpha_2'$. It can be seen that the value of h_s increases with increasing α_1' and α_2'.

4. Symmetry breaking

The characteristic property of a non-symmetric LC cell is that the place of maximal tilt angle θ_m is $z=d$ and $d\neq l/2$. The symmetry of the director distribution about the middle plane of the cell is broken. We define a dimensionless quantity Δ to describe the symmetry breaking,

$$\Delta=\frac{d-l/2}{l/2}=2\frac{d}{l}-1. \tag{38}$$

From equation (38), we see that $\Delta>0$ indicates the position of θ_m above the middle plane and $\Delta<0$ indicates the position of θ_m below the middle plane. Substituting equations (22), (23) into (38),we obtain

$$\Delta=\frac{I_{1,0}-I_{1,l}}{I_{1,0}+I_{1,l}}=\frac{I_{1,0}-I_{1,l}}{\pi h}. \tag{39}$$

We now discuss the relations between Δ and h. From the definitions of $I_{1,0}$, $I_{1,l}$ (22) and (23) as well as

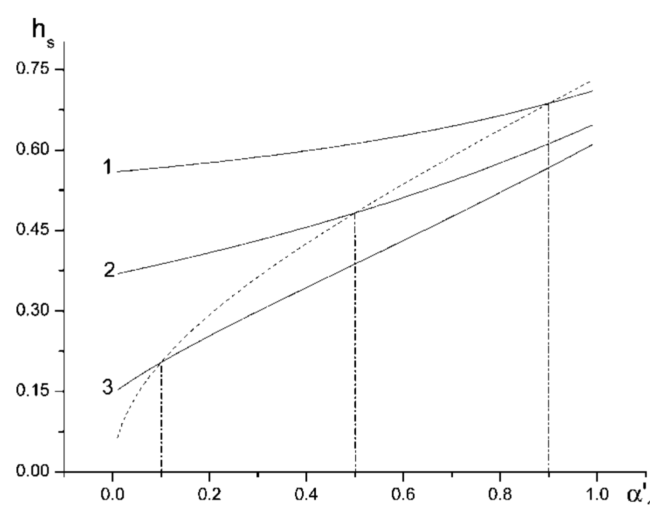

Figure 3. The $h_s-\alpha_2$ curves for various α_1'. Parameter $\gamma=0.25$. Curves 1, 2 and 3 represent $\alpha_1'=0.9$, 0.5 and 0.1, respectively. The dashed curve represents $\alpha_1'=\alpha_2'$.

Downloaded At: 17:05 25 January 2011

Downloaded At: 17:05 25 January 2011

equations (25) and (26), we see that the relations are dependent on anchoring parameters α_1, ζ_1, α_2 and ζ_2. We discuss three cases.

4.1. $h=h_{\mathrm{th}}$

In this case Δ is denoted by Δ_{th}. Because $u=0$, $I_{1,0}|_{u=0}=\cos^{-1} v_0^{\frac{1}{2}}$, $I_{1,l}|_{u=0}=\cos^{-1} v_l^{\frac{1}{2}}$, we have

$$\Delta_{\mathrm{th}}=\frac{\cos^{-1} v_0^{\frac{1}{2}}-\cos^{-1} v_l^{\frac{1}{2}}}{\pi h_{\mathrm{th}}}=\frac{\sin^{-1}\left[(1-v_0)^{\frac{1}{2}}v_l^{\frac{1}{2}}-v_0^{\frac{1}{2}}(1-v_l)^{\frac{1}{2}}\right]}{\pi h_{\mathrm{th}}}. \tag{40}$$

Substituting equations (28) and (29) into (40), leads to

$$\Delta_{\mathrm{th}}=\frac{\sin^{-1}\left\{\frac{2(\alpha_1-\alpha_2)\pi h_{\mathrm{th}}}{\left[\left(4\alpha_1^2+\pi^2h_{\mathrm{th}}^2\right)\left(4\alpha_2^2+\pi^2h_{\mathrm{th}}^2\right)\right]^{\frac{1}{2}}}\right\}}{\pi h_{\mathrm{th}}}. \tag{41}$$

Because h_{th} is itself a function of α_1 and α_2, Δ_{th} is only relevant to α_1, α_2. Using the results of h_{th} in § 3, we can calculate the value of Δ. The results are shown in figure 4, in which each of the five curves represents a relation between Δ_{th} and α_1 for fixed α_2; $\alpha_2=0.1$, 0.5, 1.0, 1.5 and 2.0 for curves 1, 2, 3, 4, and 5, respectively. We see that these curves tend to lines of small slopes when the value of α_1 is large. For the exchange of α_1 and α_2, Δ_{th} will become $-\Delta_{\mathrm{th}}$, i.e. Δ_{th} (α_1, α_2)$=-\Delta_{\mathrm{th}}$ (α_2, α_1).

4.2. $h=h_{\mathrm{s}}$

In this case Δ can be denoted by Δ_{s}. Putting $u=1$, $I_{1,0}|_{u=1}=(1+\gamma)^{\frac{1}{2}}\sinh^{-1}\left(\frac{1-v_0}{v_0}\right)^{\frac{1}{2}}$, $I_{1,l}|_{u=1}=(1+\gamma)^{\frac{1}{2}}\sinh^{-1}\left(\frac{1-v_l}{v_l}\right)^{\frac{1}{2}}$. Equation (39) leads to

$$\Delta_{\mathrm{s}}=\frac{(1+\gamma)^{\frac{1}{2}}}{\pi h_{\mathrm{s}}}\sinh^{-1}\left\{\frac{2\pi h_{\mathrm{s}}(1+\gamma)^{\frac{1}{2}}\left(\alpha_1'-\alpha_2'\right)}{\left[\pi^2h_{\mathrm{s}}^2(1+\gamma)-4\alpha_1'\right]^{\frac{1}{2}}\left[\pi^2h_{\mathrm{s}}^2(1+\gamma)-4\alpha_2'\right]^{\frac{1}{2}}}\right\} \tag{42}$$

where parameters $\alpha_1'=\alpha_1(1+2\zeta_1)$ and $\alpha_2'=\alpha_2(1+2\zeta_2)$. So Δ_{s} is a function of α_1' and α_2'.

Using the values of h_{s} in § 3, we can calculate the values of Δ_{s}. The results are shown in figure 5, in which each curve represents the relation between Δ_{s} and α_1' for fixed α_2'; and $\alpha_2'=0.1$, 1.0, 2.0, 3.0 and 4.0 respectively. We see that these curves tend to lines of small slope when the value of α_1' is large. For the exchange of α_1' and α_2', the value of Δ_{s} will become $-\Delta_{\mathrm{s}}$, i.e. $\Delta_{\mathrm{s}}\left(\alpha_1', \alpha_2'\right)=-\Delta_{\mathrm{s}}\left(\alpha_2' \alpha_1'\right)$.

4.3. $h_{\mathrm{th}}<h<h_{\mathrm{s}}$

Through much calculation, we find the relation between Δ and h is sensitive to the ratio of α_2 and α_1. Putting

$$r=\frac{\alpha_2}{\alpha_1} \tag{43}$$

and substituting equations (22), (23), (25) and (26) into (39), we can find the relation between Δ and h, which can be seen from figure 6. The typical results of

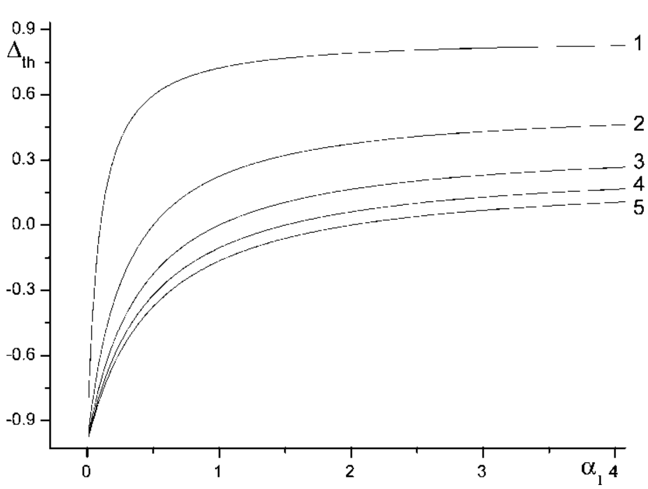

Figure 4. The $\Delta_{\mathrm{th}}-\alpha_1$ curves for various α_2 at the threshold point. Parameter $\gamma=0.25$ and curves 1, 2, 3, 4 and 5 represent $\alpha_2=0.1$, 0.5, 1.0, 1.5 and 2.0, respectively.

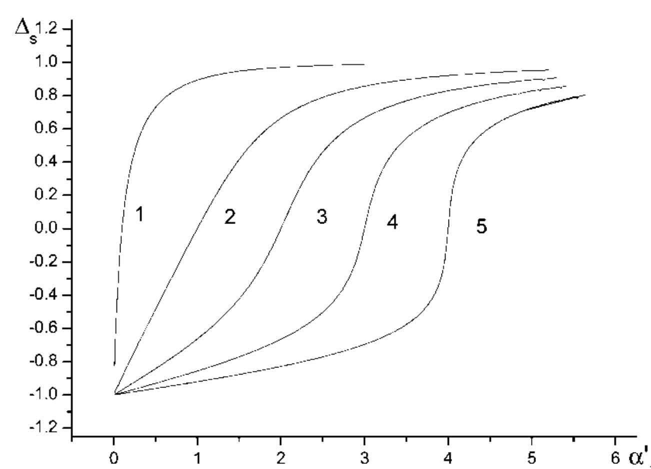

Figure 5. The $\Delta_{\mathrm{s}}-\alpha_1'$ curves for various α_2' at the saturation point. Parameter $\gamma=0.25$ and curves 1, 2, 3, 4 and 5 represent $\alpha_2'=0.1$, 1.0, 2.0, 3.0 and 4.0, respectively.

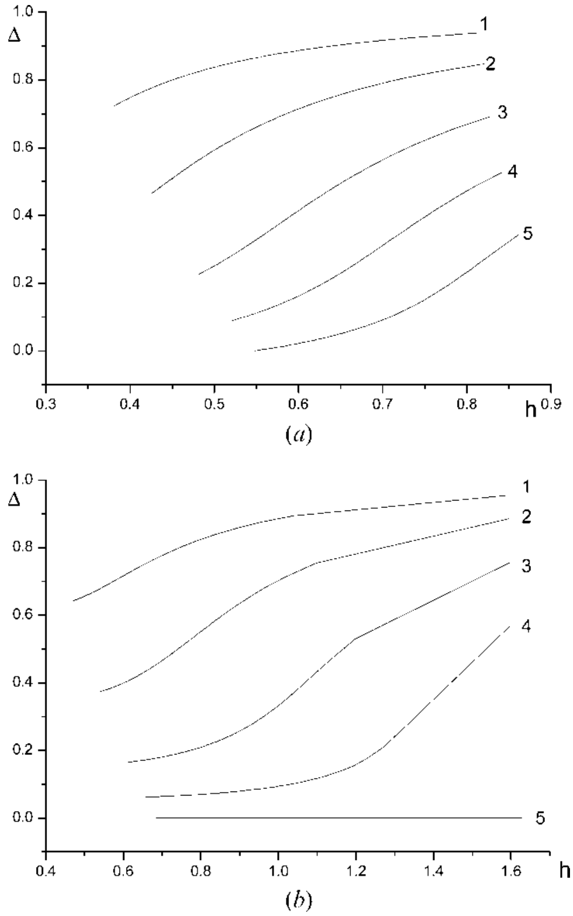

Figure 6. The $\Delta - h$ curves for various r, α_1, ζ_1, ζ_2. (*a*) Parameters $\zeta_1 = 0.2$, $\zeta_2 = 0$, $\alpha_1 = 1.0$; curves 1, 2, 3, 4 and 5 represent $r = 0.1$, 0.25, 0.5, 0.75 and 1.0, respectively. (*b*) Parameters $\zeta_1 = \zeta_2 = 0.2$, $\alpha_1 = 2.0$; curves 1, 2, 3, 4 and 5 represent $r = 0.1$, 0.25, 0.5, 0.75 and 1.0, respectively.

Downloaded At: 17:05 25 January 2011

numerical calculations are shown in figure 6 (*a*) and 6 (*b*). Five curves are denoted by 1, 2, 3, 4, and 5 for each figure. Each curve corresponds to a fixed r value; $r = 0.1$, 0.25, 0.5, 0.75 and 1.0, respectively. In figure 6 (*a*), taking $\alpha_1 = 1.0$, $\zeta_1 = 0.2$ and $\zeta_2 = 0$, we see that when $r = 1$, $\Delta \neq 0$, because $\zeta_1 \neq \zeta_2$. In figure 6 (*b*), taking $\alpha_1 = 2.0$, $\zeta_1 = 0.2$ and $\zeta_2 = 0.2$, when $r = 1$, $\Delta = 0$, because $\zeta_1 \neq \zeta_2$. From these two figures we see that Δ is also sensitive to r.

5. Measurement of anchoring strengths of a series of different substrate

Many methods are available to measure the anchoring strength A of substrates and values for many different substrates are reported [7, 8, 9]. However, there are large discrepancies between different authors, even when they have used the same method and same substrates (values differing by more than one or two orders of magnitude are often reported [10]). Hence, a standard method for measuring the anchoring strength for a series of different substrates is necessary.

We now propose a feasible experimental plan for measuring the anchoring strength. Suppose that for a certain substrate, its anchoring strength A_1 with a corresponding NLC material is well known; we can take this substrate with the NLC material as a standard combination. If another substrate has an unknown anchoring strength A_2, we can make a non-symmetric cell with the standard NLC material, for which, the bottom substrate is standard (anchoring strength A_1) and the top substrate has unknown anchoring strength A_2. Then the threshold field $H_{\rm th}$ can be measured, and A_2 can calculated.

Equation (32) leads to

$$\tan(\pi h_{\rm th}) = \frac{1}{\alpha_1} \frac{2\pi h_{\rm th}(1 + \alpha_2/\alpha_1)}{\frac{1}{\alpha_1^2}\pi^2 h_{th}^2 - 4\alpha_2/\alpha_1} \tag{44}$$

Because, $\alpha_2/\alpha_1 = A_2/A_1$, $h = \mathbf{H}/\mathbf{H}_c^0$ and $\alpha = Al/2K_{11}$ we have

$$\frac{A_2}{A_1} = H_{\rm th}(\chi_{\rm a}K_{11})^{\frac{1}{2}}\left\{(\chi_{\rm a}K_{11})^{\frac{1}{2}} H_{\rm th} \tan\left[l\left(\frac{\chi_{\rm a}}{K_{11}}\right)^{\frac{1}{2}} H_{\rm th}\right] - A_1\right\} \Bigg/ A_1\left\{A_1 \tan\left[l\left(\frac{\chi_{\rm a}}{K_{11}}\right)^{\frac{1}{2}} H_{\rm th}\right] + H_{\rm th}(\chi_{\rm a}K_{11})^{\frac{1}{2}}\right\}. \tag{45}$$

From equation (45), we can calculate the value of A_2/A_1 if l and $H_{\rm th}$ have been measured, then A_2 is obtained. Using this method, the anchoring strength for a series of different substrates can be measured. Because the anchoring strength A_1 is precisely known, and is same for each measurement, all values of anchoring strength A_2 for various substrates are comparable.

The principal advantage of this method is that the systematic error of the A_2/A_1 value can be greatly reduced. In order to explain this, by using equations (28) and (29), we express A_2/A_1 as

$$\frac{A_2}{A_1} = (v_0/1 - v_0)^{\frac{1}{2}}/(v_l/1 - v_l)^{\frac{1}{2}} \tag{46}$$

For $\mathbf{H} = H_{\rm th}$, equations (22) and (23) yield

$$\frac{\pi}{2} h_{\rm th} \frac{2d}{l} = \cos^{-1} v_0^{\frac{1}{2}} \tag{47}$$

$$\frac{\pi}{2} h_{\rm th} \frac{2l - 2d}{2l} = \cos^{-1} v_l^{\frac{1}{2}} \tag{48}$$

where d is the place of the maximal tilt angle $\theta_{\rm m}$ at the threshold point. From equations (47), (48) and (38), we obtain

$$\left(\frac{v_0}{1-v_0}\right)^{\frac{1}{2}} = \cot\left(\frac{\pi}{2}h_{\rm th}\frac{2d}{l}\right) = \cot\left[\frac{l}{2}\left(\frac{\chi_{\rm a}}{K_{11}}\right)^{\frac{1}{2}}H_{\rm th}(1+\Delta_{\rm th})\right] \quad (49)$$

$$\left(\frac{v_l}{1-v_l}\right)^{\frac{1}{2}} = \cot\left(\frac{\pi}{2}h_{\rm th}\frac{2l-2d}{l}\right) = \cot\left[\frac{l}{2}\left(\frac{\chi_{\rm a}}{K_{11}}\right)^{\frac{1}{2}}H_{\rm th}(1+\Delta_{\rm th})\right]. \quad (50)$$

Substituting equations (49) and (50) into equation (46), leads to

$$\frac{A_2}{A_1} = \frac{\tan\left[\frac{l}{2}\left(\frac{\chi_{\rm a}}{K_{11}}\right)^{\frac{1}{2}}H_{\rm th}(1-\Delta_{\rm th})\right]}{\tan\left[\frac{l}{2}\left(\frac{\chi_{\rm a}}{K_{11}}\right)^{\frac{1}{2}}H_{\rm th}(1+\Delta_{\rm th})\right]}. \quad (51)$$

Equation (51) is another formula of relative anchoring strength A_2/A_1, and includes the parameter $\Delta_{\rm th}$. From figure 4, we can see that $\Delta_{\rm th}$ is independent of l when $\alpha_1>1$. We can obtain $\alpha_1>1$ by adjusting the thickness l of the NLC cell for $\alpha=Al/2K_{11}$. The change of $\Delta_{\rm th}$ is only 10^{-3} when the change of l is 10^{-2}.

By means of equation (51), we analyse the measurement error of A_2/A_1. The original experimental measured values are l and $H_{\rm th}$; many reasons may cause the error of measured values of these quantities, such as the following.

(1) Experimental environment. There is evidence to illustrate that the anchoring strength A is dependent on temperature [1].
(2) The NLC cell fabrication, i.e. whether the two substrates are strictly plane and parallel, and whether the easy direction **e** occurs on the two substrates (the pretilt angle is zero).
(3) Measurement techniques.

These factors all influence the measurement of l and $H_{\rm th}$. However, from equation (51), we can see that errors in l and $H_{\rm th}$ influence the values of numerator and denominator in the same way. So errors in A_2/A_1 can be counteracted. We therefore believe that any large discrepancy in measured values of anchoring strength, can probably be eliminated by this method.

References

[1] SONG, A., 1995, *The Surface Physics Of Liquid Crystal* (Gorden and Breach).
[2] RAPINI, A., and PAPOULAR, M., 1969, *J. Phys. (Paris) Colloq.*, **30,** C4–54.
[3] FRANK, F. C., 1958, *Discuss. Faraday Soc.*, **25,** 19.
[4] ELSGOTS, L., 1980, *Differential Equations and Variation Calculus* (Moscow: MIR); Smirnov, V., 1975, *Caurs de Mathematiques Superieures IV* (Moscow: MIR).
[5] GUOCHEN, Y., JIANRU, S., and YING, L., 2000, *Liq. Cryst.*, **27,** 875.
[6] GUOCHEN, Y., and SUHUA, Z., 2002, *Liq. Cryst.*, **29,** 641.
[7] SHOHEI, N., 1978, *Appl. Phys. Lett.*, **33,** 1.
[8] SHOHEI, N., 1980, *J. Appl. Phys.*, **51,** 12.
[9] ANDRIENKO, D., DYADYUSHA, A., ILJIN, A., KURIOZ, YU., and REZNIKOV, YU., 1998, *Mol. Cryst. liq. Cryst.*, **321,** 271.
[10] SUGINURA, A., MATSUMOTO, K., ZHANG CHAN, O.-Y., and IWEUNOTO, M., 1996, *Phys. Rev. E*, **54,** 5217.

Downloaded At: 17:05 25 January 2011